

Scaling Applications in Fire Research*

James G. Quintiere

Center for Fire Research, National Engineering Laboratory, National Bureau of Standards, US Department of Commerce, Gaithersburg, Maryland 20899, USA

(Received 26 August 1988; revised version received and accepted 8 December 1988)

ABSTRACT

The principles for scaling fire phenomena are examined from the dimensionless groups derived from the governing differential equations. A review of the literature shows examples of where correlations have been successfully developed for a wide range of fire phenomena in terms of the significant dimensionless groups. Scaling techniques based on Froude modeling, pressure modeling and analog modeling are described and illustrated. The use of small geometric models ranging from fire plumes to enclosure fires are illustrated by many examples.

NOTATION

a	Pressure ratio
A	Area
b	Stick thickness
c, c_p, c_v	Specific heats
D	Diameter
D_i	Diffusion coefficient
f	Function
g	Gravitational acceleration
h	Heat transfer coefficient

* Paper presented at the International Symposium on Scale Modeling, 18-22 July 1988, Tokyo, Japan.

This paper is a contribution of the National Bureau of Standards and is not subject to copyright.

H	Height
I	Radiant intensity
k	Thermal conductivity
l	Length scale
L	Heat of gasification
L_f	Flame height
m	Mass
p	Pressure
P	Crib porosity
q	Heat
Q	Chemical energy
r	Stoichiometric air to fuel mass ratio
r	Radius
R	Gas constant
t	Time
T	Temperature
u	Velocity
V	Velocity scale
x	Coordinate variable
Y_i	Specie i mass fraction
z	Vertical coordinate variable

Greek letters

α	Constant in t^2 -fire
δ	Solid thickness
ΔH	Heat of combustion
ω	Solid angle
κ	Absorption coefficient
μ	Viscosity
σ	Stefan-Bolzman constant
ρ	Density
τ	Time scale
ζ	Equation (24)
η	z/l

Subscripts

a	Ambient
ext	External
f	Flame
i	Specie
m	Model
o	Initial opening

p	Prototype
r	Radiation
s	Solid, surface

Superscripts

($\hat{\quad}$)	Dimensionless variables
($\dot{\quad}$)	Per unit time
($\ddot{\quad}$)	Per unit area
($\overset{\circ}{\quad}$)	Per unit volume

INTRODUCTION

The study of fire phenomena in reduced-scale systems has been a pursuit of expedience and scientific strategy. It is apparent that accidental fires in the built and natural environments occur at a physical scale to prohibit their experimental study at realistic scales. Furthermore, the complexities of fire preclude complete mathematical solutions to its problems. Consequently, a deliberate strategy of scale modeling, based on the governing laws of physics, is both an essential and practical means of obtaining general results. The use of dimensional analysis leading to the significant dimensionless parameters is a well known technique for generalizing experimental results and for establishing the 'laws of scaling' for a system. The study of a fire phenomena at a scale suitable for laboratory observation can also give insight on the mechanisms and behavior of the system, even if it does not give exact quantitative results.

Thomas¹ refers to a scale model study (at 1/3 and 1/10-scale) of the Austrian Ring Theater disaster in 1906 to help explain that fire. The benefits of that study have been lost in time, but it should certainly provoke the thought of scale model studies for fire investigations. Thomas¹ also cites the use of a water-salt water analog scaling study for a factory fire displayed at the Rote Hahn Exhibition in Cologne in 1961.

For a comprehensive presentation of the theoretical bases for scaling in fire, the reader is referred to Williams² who derives all of the apparent dimensionless groups (more than 28 independent π -parameters). He also discusses various strategies for scaling in fire. A previous review, which demonstrates the use of scaling for various fire problems, was given by Heskestad in 1975.³ This paper will present a simplified theoretical basis for scaling, in the style of Williams,² and show how those general results apply to a variety of applications. In this

review, examples will be cited which range from fire plumes to building fires, and different scaling techniques will be illustrated. In all cases, despite a theoretical basis, the scaling will be incomplete since it is not possible to adequately address or include all of the variables present in the problem. Consequently, scaling in fires is an art which requires attention to ignored phenomena and adequate proof and demonstration that the scaling technique is proper. Hottel⁴ presents a good discussion on fire modeling and the trade-offs one is forced to make, particularly with respect to radiant heat transfer effects.

GOVERNING EQUATIONS AND DIMENSIONLESS GROUPS

The scaling laws that apply to different fire phenomena can all be traced back to the governing differential conservation equations. The equations selected will not be comprehensive since some phenomena will be excluded because of their general unimportance. For example, diffusion flames do not generally depend on chemical kinetics, and thermo-diffusion effects and viscous dissipation are insignificant. Also, without a loss in generalization, only the one-dimensional form of the equations will be presented.

Mass

$$\frac{\partial \rho}{\partial t} + \frac{\partial(\rho u)}{\partial x} = 0 \quad (1)$$

Momentum (vertical)

$$\rho \frac{\partial u}{\partial t} + u \frac{\partial \rho}{\partial x} = -\frac{\partial p'}{\partial x} + g(\rho_a - \rho) + \frac{4}{3}\mu \frac{\partial^2 u}{\partial x^2} \quad (2)$$

where

$$p' = p - p_a \quad (3a)$$

$$\frac{dp_a}{dx} = -\rho_a g \quad (3b)$$

and p_a is the ambient pressure distribution.

Energy

$$\rho c_p \left(\frac{\partial T}{\partial t} + u \frac{\partial T}{\partial x} \right) = k \frac{\partial^2 T}{\partial x^2} - 4\kappa\sigma T^4 + \int_0^{4\pi} \kappa I d\omega + \dot{Q}''' + \frac{\partial p}{\partial t} \quad (4)$$

Radiative Transfer Equation

$$\frac{dI}{dx} = -\kappa \left(I - \frac{\sigma T^4}{\pi} \right) \quad (5)$$

***i*th Specie**

$$\rho \left(\frac{\partial Y_i}{\partial t} + u \frac{\partial Y_i}{\partial x} \right) = \frac{\partial}{\partial x} \left(\rho D_i \frac{\partial Y_i}{\partial x} \right) + \dot{m}_i''' \quad (6)$$

State

$$p = R\rho T \quad (7)$$

Solid Energy

$$\left(\frac{\rho c}{k} \right)_s \frac{\partial T_s}{\partial t} = \frac{\partial^2 T_s}{\partial x^2} \quad (8)$$

Energy Boundary Condition, $x = 0$

(x is positive into the gas phase)

$$k \frac{\partial T}{\partial x} = \dot{m}'' L - \left[\dot{q}_{r,f}'' + \dot{q}_{r,ext}'' - \sigma T_s^4 - k_s \frac{\partial T_s}{\partial x} + \dot{m}'' c_s (T_s - T_o) \right] \quad (9)$$

where heat of gasification, $L \equiv \Delta h_{\text{vap}} + c_s(T_s - T_o)$, $\dot{q}_{r,f}''$ is the flame radiative heat flux $(1 - e^{-\kappa x})\sigma T_f^4$, $\dot{q}_{r,ext}''$ is the external radiative heat flux σT_{ext}^4 , σT_s^4 is the surface reradiative heat flux, and T_f is the flame temperature, T_{ext} is the representative surface temperature of the surrounding surface, and κ is the absorption coefficient proportional to ρY_i for absorbing species, and is also dependent on T .

The above equations can be made dimensionless by introducing the following normalizing parameters:

$$\left. \begin{array}{l} \text{Geometric length scale } l \\ \text{Material thickness } \delta \\ \text{Characteristic velocity } V \\ \text{Characteristic time } \tau \\ \text{Initial or ambient quantities } T_o, \rho_o, \rho_o \\ \text{Characteristic pressure defect } p_* \end{array} \right\} \quad (10)$$

The dimensionless variables denoted by ($\hat{\quad}$) with their resulting dimen-

dimensionless coefficients (π groups) are presented below:

Mass

$$\pi_1 \frac{\partial \hat{\rho}}{\partial \hat{t}} + \frac{\partial(\hat{\rho}\hat{u})}{\partial \hat{x}} = 0 \quad (11)$$

Momentum

$$\hat{\rho} \left(\pi_1 \frac{\partial \hat{u}}{\partial \hat{t}} + \hat{u} \frac{\partial \hat{u}}{\partial \hat{x}} \right) = -\pi_2 \frac{\partial \hat{p}'}{\partial \hat{x}} + \frac{4}{3} \pi_3 \frac{\partial^2 \hat{u}}{\partial \hat{x}^2} + \pi_4 (1 - \hat{\rho}) \quad (12)$$

Energy

$$\begin{aligned} \hat{\rho} \left(\pi_1 \frac{\partial \hat{T}}{\partial \hat{t}} + \hat{u} \frac{\partial \hat{T}}{\partial \hat{x}} \right) &= \pi_5 \pi_3 \frac{\partial^2 \hat{T}}{\partial \hat{x}^2} + \hat{Q} \\ &+ \pi_6 \frac{\partial \hat{p}}{\partial \hat{t}} + [\pi_7 \pi_8 / (\pi_3 \pi_5)] \left[\int_0^{4\pi} \hat{I} d\omega - 4\hat{T}^4 \right] \end{aligned} \quad (13)$$

Specie

$$\hat{\rho} \left(\pi_1 \frac{\partial Y_i}{\partial \hat{t}} + \hat{u} \frac{\partial Y_i}{\partial \hat{x}} \right) = \pi_9 \frac{\partial}{\partial \hat{x}} \left(\hat{\rho} \frac{\partial Y_i}{\partial \hat{x}} \right) + \hat{M}_i \quad (14)$$

State

$$\hat{p} = [(1 - \pi_{10}) / \pi_6] \hat{\rho} \hat{T} \quad (15)$$

Solid Energy

$$\pi_{11} \frac{\partial \hat{T}_s}{\partial \hat{t}} = \frac{\partial^2 \hat{T}_s}{\partial \hat{x}_s^2} \quad (16)$$

Boundary Condition

$$\frac{\partial \hat{T}}{\partial \hat{x}} = \frac{\pi_{12} \hat{m}}{\pi_5} - \pi_8 (\pi_7 \hat{x}_i \hat{T}_i^4 + \hat{T}_{\text{ext}}^4 - \hat{T}_s^4) + \pi_{13} \frac{\partial \hat{T}_s}{\partial \hat{x}_s} - \pi_{14} (\hat{T}_s - 1) \quad (17)$$

The following dependent dimensionless variables are defined:

$$\begin{aligned} \hat{Q} &= \frac{\dot{Q}''' l}{\rho_o V c_p T_o} \\ \hat{M}_i &= \frac{\dot{m}_i''' l}{\rho_o V} \\ \hat{m} &= \frac{\dot{m}''' l}{\mu} \\ \hat{I} &= \frac{I}{\sigma T_o^4} \end{aligned} \quad (18)$$

and no additional π -groups are introduced from the radiative transfer equation. The independent π -groups are given below. In some cases

equating a π to 1 allows us to determine a characteristic normalizing parameter in terms of other variables; thus, this procedure effectively eliminates that π . Also, some of the π groups are related to more common dimensionless groups, and these will be noted below.

Dimensionless Groups:

$$\pi_1 = \frac{l}{V\tau} = 1, \quad \tau = \frac{l}{V}$$

$$\pi_2 = \frac{p^*}{\rho_o V^2} = 1, \quad p^* = \rho_o V^2$$

$$\pi_3 = \frac{\mu}{\rho_o V l} = \frac{1}{\text{Re}} \quad \text{where Re is the Reynolds number}$$

$$\pi_4 = \frac{gl}{V^2} = \frac{1}{\text{Fr}^2} \quad \text{where Fr is the Froude number}$$

$$\pi_5 = \frac{k}{\mu c_p} = \frac{1}{\text{Pr}} \quad \text{where Pr is the Prandtl number}$$

$$\pi_6 = \frac{lp^*}{\rho_o c_p V T_o \tau} = \frac{lV}{c_p T_o l/V} = \frac{V^2}{c_p T_o}$$

$$\pi_7 = \kappa l$$

$$\pi_8 = \frac{\sigma T_o^3 l}{k}$$

$$\pi_9 = \frac{\rho_o D_i}{\mu} = \frac{1}{\text{Sc}} \quad \text{where Sc is the Schmidt number}$$

$$\pi_{10} = c_v/c_p$$

$$\pi_{11} = \frac{\rho_s c_s \delta^2}{k_s \tau}$$

$$\pi_{12} = \frac{L}{c_p T_o}$$

$$\pi_{13} = \frac{k_s/\delta}{k/l}$$

$$\pi_{14} = \frac{c_s}{c_p}$$

MODELING APPROACHES

Three modeling strategies have been effectively used in fire research. Each is incomplete since no practical strategy allows for matching all of the π -groups. Yet these partial scaling techniques have produced good quantitative results and insight into fire phenomena at an advantage of scale and cost. Examples of the three strategies will be given, but for now they are summarized as below.

1 Froude modeling

The experiments are performed in air at normal ambient conditions with π_4 the primary group preserved. For natural convection π_4 is set equal to 1 so that $V = \sqrt{gl}$ is the characteristic velocity. It is assumed that solid boundary effects are nonexistent or unimportant in order to justify ignoring π_3 or the Reynolds number. It will not be possible to preserve all of the radiation and conduction groups ($\pi_7, \pi_8, \pi_{12}, \pi_{13}$) and various approximations have been made to attempt their partial accommodation. For example, a consideration of pure heat transfer at a solid boundary might include convection heat transfer explicitly as

$$\frac{\partial \hat{T}}{\partial \hat{x}} = \text{Nu} (\hat{T} - \hat{T}_s) \quad \text{where} \quad \text{Nu} = \frac{hl}{\kappa} \quad (19)$$

with Nu, the Nusselt number. It could be represented for turbulent convection as

$$\text{Nu} = 0.036 \text{Pr}^{1/3} \text{Re}^{0.8} \quad (20)$$

Substituting eqn. (19) into (17) yields a modified set of groups for pure heat transfer

$$(\pi_7 \hat{x}_f \hat{T}_f^4 + \hat{T}_{\text{ext}}^4 - \hat{T}_s^4) + \frac{\pi_{13}}{\pi_8} \frac{\partial \hat{T}_s}{\partial \hat{x}_s} = \frac{\text{Nu}}{\pi_8} (\hat{T} - \hat{T}_s) \quad (21)$$

where

$$\frac{\pi_{13}}{\pi_8} = \frac{k_s}{\sigma T_o^3 \delta} \quad \text{and} \quad \frac{\text{Nu}}{\pi_8} = \frac{h}{\sigma T_o^3}$$

By proper choice of the solid boundary materials, it is possible to partially preserve some of the boundary heat transfer effects even though Re is explicitly ignored in 'Froude scaling'.

An extension of Froude modeling is used often with success for purely natural convection conditions (indicative of most fire situations) if the Boussinesq assumption is invoked, i.e.

$$1 - \hat{\rho} = \hat{T} - 1 \quad (22)$$

in eqn. (12) and $\hat{\rho} = 1$ in all other terms. Furthermore, although \hat{Q} and \hat{M}_i are dependent variables, it is often of value to consider these as known source terms. This is especially used when we wish to model effects 'far' from the combustion region. In this case a 'point source' representation is used with \hat{Q} and \hat{m}_i , the energy and specie production rates respectively. In this case, a new normalized temperature (and mass fraction) is derived as follows

$$\pi_4(1 - \hat{\rho}) = (\pi_4 \zeta) \left(\frac{\hat{T} - 1}{\zeta} \right) = \frac{\hat{T} - 1}{\zeta} \quad (23)$$

Hence,

$$\zeta = \frac{V^2}{g l} \quad (24)$$

Furthermore, it is possible to explicitly eliminate the \hat{Q} and \hat{M}_i terms by introducing ζ into eqns. (13) and (14) and letting

$$\frac{\hat{Q}}{\zeta} = \frac{\hat{M}_i}{\zeta} = 1 \quad (25)$$

and with

$$\hat{Q} = \frac{(\hat{Q}/l^3)l}{\rho_o V c_p T_o} \quad (26)$$

it follows from eqn. (24) that

$$V = \left(\frac{g \hat{Q}}{\rho_o c_p T_o l} \right)^{1/3} \quad (27a)$$

or

$$V = \left(\frac{g \hat{m}_i}{\rho_o l} \right)^{1/3} \quad (27b)$$

alternatively from eqn. (18). Note that the specie concentrations and temperature fields will be similar under conditions of no solid conduction or radiative losses, and can be related provided the stoichiometry is known.

2 Analog modeling

The fire flow effects are modeled by using different fluids to simulate the buoyancy effects. For example, the Froude modeling criteria could be applied to fire induced flows, but the medium in the reduced-scale system could be water. The smaller kinematic viscosity of water, compared to air has the added advantage of assuring high Reynolds conditions (turbulence) for the reduced-scale water system. In the water system another fluid or a solute (e.g. salt) could be used to

simulate a heat source in the fire system. In that case, the mass, momentum and specie equations in the water system correspond to the mass, momentum and energy (and specie) equations of the fire system.

3 Pressure modeling

A way to preserve the π -groups in Froude modeling as well as the Re can be accomplished by changing the pressure of the ambient in the model. For example, let us require the equivalence of \hat{T} in the model and the prototype (p). Then from

$$p_o = R\rho_o T_o$$

and recognizing that μ , c_p , k , $\rho_o D_i$ and Y_i are also invariant, it follows that for the pressure ratio, a

$$a \equiv \frac{p_{o,m}}{p_{o,p}} = \frac{\rho_{o,m}}{\rho_{o,p}} \quad (28)$$

by preserving π_3 and π_4

$$\frac{V_m}{V_p} = a^{-1/3} \quad (29)$$

$$\frac{l_m}{l_p} = a^{-2/3} \quad (30)$$

and from π_1

$$\frac{\tau_m}{\tau_p} = a^{-1/3} \quad (31)$$

From the definition of \hat{m} , eqn. (18) and eqn. (30), it follows that scaling must require

$$\frac{\dot{m}_m''}{\dot{m}_p''} = a^{2/3} \quad (32)$$

for the burning rate of a solid (or liquid) fuel. Thus, eqns. (29–32) give the behaviour of these variables with the pressure ratio, a .

Examples using the three modeling strategies will be illustrated for a number of fire problems.

FIRE PLUME

The characteristics of fire plumes have not been solved exactly from the basic equations. Nevertheless, approximate and partial solutions have been obtained, but the most credible results come from correlations of data. These correlations have been developed and enhanced by scaling

and dimensional analysis techniques. Let us consider that radiation effects are negligible, the flow is steady, and viscous effects are unimportant for this free boundary fire plume problem. Hence, Froude modeling applies, and furthermore let us invoke the Boussinesq assumption. Since no apparent length scale is evident in this problem, let us modify our analysis beginning at eqn. (23) by letting $\zeta = 1$ and determining a reference length. By setting eqns. (24) and (26) to 1, it follows that

$$l = \left(\frac{\dot{Q}}{\rho_o \sqrt{g} c_p T_o} \right)^{2/5} \quad (33)$$

$$V = \sqrt{g} \left(\frac{\dot{Q}}{\rho_o \sqrt{g} c_p T_o} \right)^{1/5} \quad (34)$$

are the derived length and velocity scales. As a consequence it follows that from the governing equations, (11)–(13), the centerline plume temperature and velocity are

$$\frac{T - T_o}{T_o} = f_1\left(\frac{z}{l}\right) \quad (35)$$

and

$$u = \sqrt{g} \left(\frac{\dot{Q}}{\rho_o \sqrt{g} c_p T_o} \right)^{1/5} f_2\left(\frac{z}{l}\right) \quad (36)$$

where z is the vertical coordinate with l given by eqn. (33), and f_1 and f_2 imply specific functional dependence. Although the severe restriction of the Boussinesq assumption has been used here, McCaffrey⁵ finds

$$\frac{u}{V} \sim \eta^{1/2} \quad \text{and} \quad \frac{T - T_o}{T_o} \sim \eta^0; \quad \left(\eta \equiv \frac{z}{l} \right) \quad (37)$$

in the combusting region; and

$$\frac{u}{V} \sim \eta^{-1/3} \quad \text{and} \quad \frac{T - T_o}{T_o} \sim \eta^{-5/3} \quad (38)$$

in the far field noncombusting plume region. Equation (38) can be deduced from the point source buoyant plume solution as reported by Taylor⁶ and shown to hold for a wide range of pool fire conditions by Yokoi.⁷ McCaffrey⁸ has also shown the results of eqns. (37) and (38) hold for very large pool fires (30 m diameter), but it underestimates temperatures in the combusting region due to apparent radiation effects. For example, the correlation for velocity is shown in Fig. 1.⁵

The dimensionless groups governing the height of the flame (L_f) for a fire of base diameter D can be estimated from eqn. (37). Assuming that

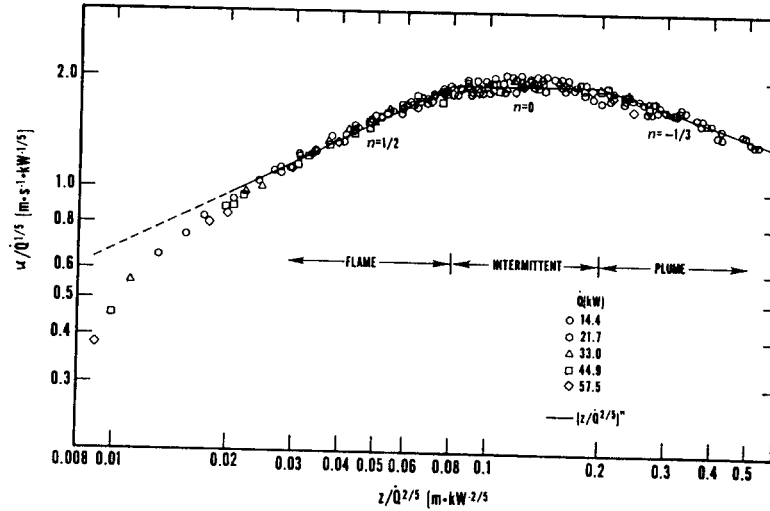


Fig. 1. Vertical centreline velocity (from McCaffrey⁵).

all of the fuel reacts with stoichiometric air up to the flame tip, and the fuel supply is small compared to the air entrained, we can write in dimensional terms

$$\dot{m}_f r \sim \int \rho u \, dA \sim \rho_o V \left(\frac{z}{l} \right)^{1/2} DL_f, \quad z \sim L_f \quad (39)$$

where \dot{m}_f is the fuel supply rate and r is the stoichiometric air to fuel ratio. Substituting for V and l (eqns. 33 and 34), and noting that $\dot{Q} = \dot{m}_f \Delta H$ where ΔH is the heat of combustion, it can be shown that

$$\frac{L_f}{D} \sim \left(\frac{\dot{Q}}{\sqrt{g} \rho_o c_p T_o D^{5/2}} \right)^{2/3} \left(\frac{c_p T_o}{\Delta H / r} \right)^{2/3}$$

which identifies the dimensionless groups. Heskestad⁹ has shown that for a wide range of fuels and fire sizes

$$\frac{L_f}{D} = -1.02 + 15.6 \left[\left(\frac{c_p T_o}{\Delta H / r} \right)^3 \left(\frac{\dot{Q}}{\sqrt{g} \rho_o c_p T_o D^{5/2}} \right)^2 \right]^{1/5} \quad (40)$$

is a best fit to the data.

An impressive example of modeling fire plume phenomena was done by Emori and Saito.¹⁰ They used a form of Froude modeling to reproduce a fire whirl which occurred in an actual forest fire. The terrain was modeled at a scale of 1/2500, and wind was generated by a wind tunnel.

CEILING JETS

In a study of an axisymmetric jet produced by a fire beneath a ceiling, Alpert¹¹ was able to demonstrate maximum temperature and velocity correlations for a wide range of fire configurations. The scaling variables follow from Froude modeling (eqns. (23-27)) with $l = H$, the distance of the fire to the ceiling. With the coordinates z (vertical), r (radial), the ceiling jet temperature and velocity should follow the functional form

$$\frac{T - T_o}{T_o} \frac{gH}{\left(\frac{g\dot{Q}}{\rho_o c_p T_o H}\right)^{2/3}} = f_3\left(\frac{r}{H}, \frac{z}{H}\right) \tag{41}$$

$$\frac{u}{(g\dot{Q}/\rho_o c_p T_o H)^{1/3}} = f_4\left(\frac{r}{H}, \frac{z}{H}\right) \tag{42}$$

	\dot{Q} (Btu/min)	D (ft)	H (ft)	Reference
△	4.67	0.33	1.58-4.1	MILLER
○	3.36	0.33	1.58-4.1	MILLER
□	2.0	0.33	1.58-4.1	MILLER
●	15,000	1.6	15	THOMPSON
■	40,000	2.5	15	THOMPSON
◐	80,000	3.4	15	THOMPSON
▲	150,000	4.4	15	THOMPSON

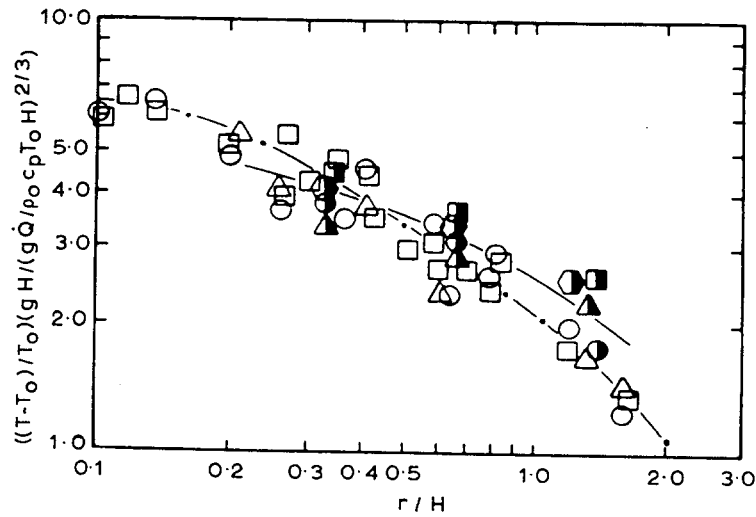


Fig. 2. Dimensionless near maximum ceiling jet temperature increase (from Alpert¹¹).

An example of the results for the maximum temperature are shown in Fig. 2.¹¹

Heskestad and Delichatsios¹² examined the transient characteristics of ceiling jets due to fires. They considered power-law fires, e.g. $\dot{Q} = \alpha t^2$, finding the second-power representative of most fires. Selecting the characteristic time $\tau = l/V$, and using Froude modeling as developed in eqns. (41) and (42), the t^2 -fire has the following dimensionless variables

$$\tau = \frac{H}{\left(\frac{g\dot{Q}}{\rho_o c_p T_o H}\right)^{1/3}} = \frac{H}{\left(\frac{g\alpha\tau^2}{\rho_o c_p T_o H}\right)^{1/3}}$$

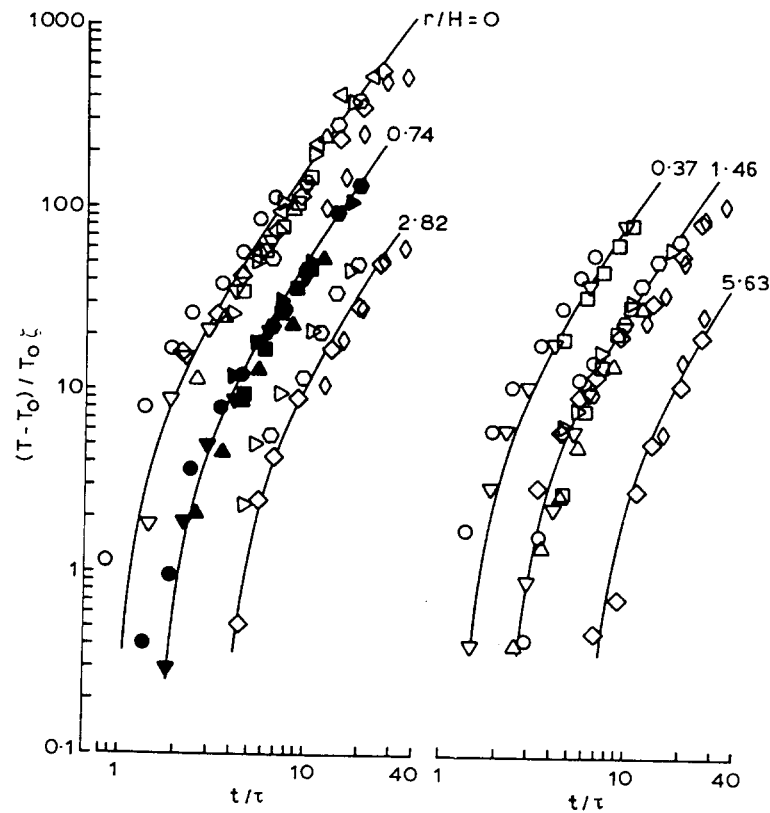


Fig. 3. Dimensionless unsteady ceiling jet temperature rise as a function of time at a fixed position z/H from (12), ζ by eqn. (45). \circ , $\alpha = 42.6 \text{ W/s}^2$, $H = 7.91 \text{ m}$; ∇ , $\alpha = 11.7 \text{ W/s}^2$, $H = 8.50 \text{ m}$; \square , $\alpha = 2.98 \text{ W/s}^2$, $H = 8.64 \text{ m}$; \triangle , $\alpha = 42.6 \text{ W/s}^2$, $H = 3.65 \text{ m}$; \triangleleft , $\alpha = 11.7 \text{ W/s}^2$, $H = 4.23 \text{ m}$; \odot , $\alpha = 2.98 \text{ W/s}^2$, $H = 4.37 \text{ m}$; \diamond , $\alpha = 11.7 \text{ W/s}^2$, $H = 2.10 \text{ m}$; \diamond , $\alpha = 2.98 \text{ W/s}^2$, $H = 2.24 \text{ m}$. (Filled symbols used for clarity in data segregation.)

or

$$\tau = H^{4/5} \left(\frac{g}{\rho_o c_p T_o} \right)^{-1/5} \alpha^{-1/5} \quad (43)$$

and it follows that

$$\frac{T - T_o}{T_o \zeta} = f_5 \left(\frac{z}{H}, \frac{r}{H}, \frac{t}{\tau} \right) \quad (44)$$

where here

$$\begin{aligned} \zeta &= \left(\frac{g \dot{Q}}{\rho_o c_p T_o H} \right)^{2/3} / gH \\ &= \left(\frac{g \alpha \tau^2}{\rho_o c_p T_o H} \right)^{2/3} / gH \\ \zeta &= \left(\frac{g}{\rho_o c_p T_o} \right)^{2/5} \alpha^{2/5} gH^{-3/5} \end{aligned} \quad (45)$$

An expression for the velocity results can be derived in a similar manner. An example of the scaling results for temperature at a fixed z/H is shown in Fig. 3 from the study by Heskestad and Delichatsios.¹²

BURNING (PYROLYSIS) RATE

The simply-stated problem of predicting the rate of burning of a fully involved solid or liquid fuel is too complex to permit a general solution. It depends not only on the fuel, but its configuration, orientation and environmental conditions. From the governing equations (11)–(15) and the pyrolysis (evaporative) boundary condition (9), it can be shown that the spatially-averaged steady mass loss rate would depend on the following π -groups

$$\frac{\dot{m}'' l}{\mu} = f_6 \left(\frac{k}{\mu c_p}, \frac{L}{c_p T_o}, \frac{\sigma T_o^3 l}{k}, \kappa l, \frac{(\mu/\rho_o)^2}{gl^3} \right) \quad (46)$$

where π_4 and π_2 have been set equal to 1 in order to define V and p^* . Note that the source terms \dot{Q} and \dot{M}_i in the energy and specie equations can be eliminated by introducing the Shvab-Zeldovich variables and do not explicitly appear in eqn. (46) provided chemical kinetic effects are unimportant.

Pressure modeling has been used to examine the burning rates of various fuels and their configurations with good success.^{13–16} For geometric similarity in the fuel, and with negligible radiation effects, eqn. (46) suggests

$$\frac{\dot{m}'' D}{\mu} = f_7 \left(\frac{D}{l}, \frac{\rho_o^2 g l^3}{\mu^2} \right) \quad (47)$$

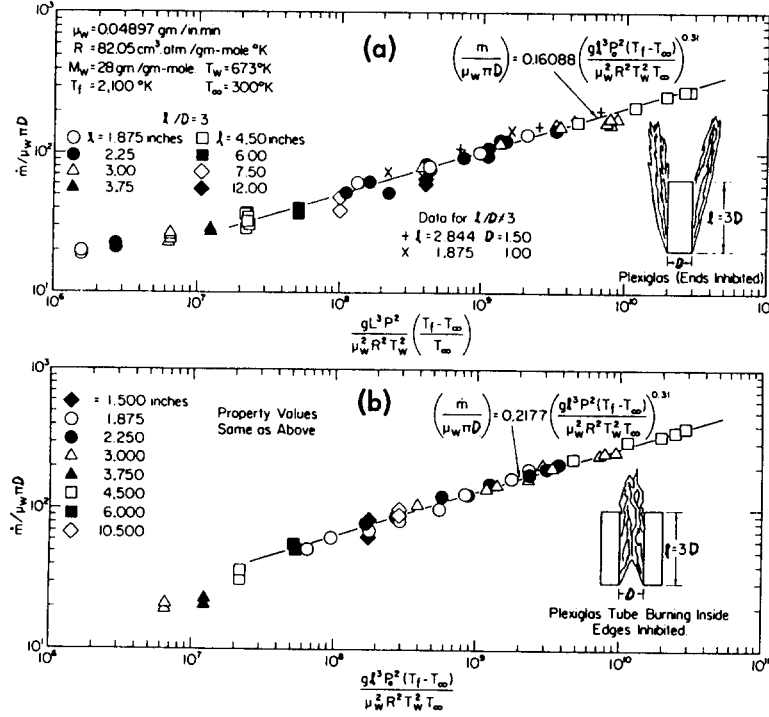


Fig. 4. Mass burning rate in pressure modeling for vertical cylinders and tubes (from deRis *et al.*¹³).

As discussed previously, the conditions for pressure modeling would hold T (and thermal properties) invariant, with $\rho_o = p_o / RT_o$ so that $\rho_o^2 l^3$ invariant requires $l \propto p_o^{-2/3}$. Figure 4 shows the results of deRis *et al.*¹³ for several scales at different ambient pressures. These results for turbulent burning at fuel heights as small as 1.5 inches confirm the viability of pressure modeling. In these studies the Grashof number (Gr) has been used in place of the second π -term in eqn. (47) by introducing the temperature ratio $(T_f - T_o) / T_o$ where T_f is an assigned flame temperature

$$Gr = \frac{g l^3 (p_o / RT_o)^2 (T_f - T_o)}{\mu^2} \left(\frac{T_f - T_o}{T_o} \right) \quad (48)$$

By examining the boundary condition eqn. (17) one can recognize that $\dot{m}'' l / \mu$ has the following dependences with respect to heat transfer

$$\pi_8 \pi_7 \sim \text{flame radiation} \sim p_o l^2, \text{ since } \kappa \sim p_o$$

$$\pi_8 \sim \text{surface reradiation} \sim l^1$$

$$1 \sim \text{convective heat transfer} \sim p_o^0 l^0$$

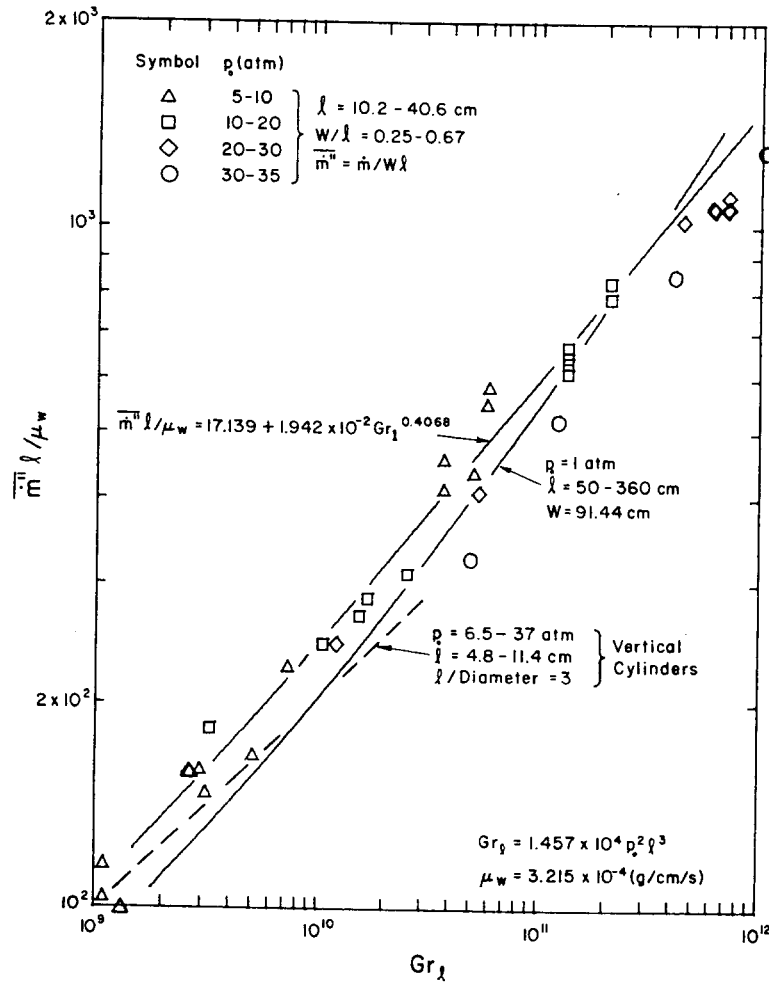


Fig. 5. Mass burning rate in pressure modeling for vertical walls (from Alpert¹⁵).

and flame radiation and surface reradiation have opposite signs. Pressure modeling does not preserve radiative effects as it does convective heat transfer; thus we would expect some trouble with this approach in modeling large fires for which radiative effects are significant. Alpert¹⁵ found that despite these limitations, pressure modeling appears to work well for wall fires up to 360 cm, or pool fires of less than 50 cm, in diameter. Apparently, compensation between flame and surface radiation terms contribute to this success. Figure 5 shows Alpert's results for wall fires.

Alpert¹⁶ also showed wood crib (ordered-stick-array) burning rates could be modeled using the pressure scaling criterion based on

convective dominated burning. From eqn. (32) we expect

$$(\dot{m}'' p_o^{-2/3})_m = (\dot{m}'' p_o^{-2/3})_p \tag{49}$$

and we reason that

$$\frac{\dot{m}'' l}{\mu} = f_3(t/\tau) \tag{50}$$

for the crib with τ selected as a characteristic burnout time for the wood, i.e.

$$\tau = \frac{\rho_s l}{\dot{m}''} \sim \frac{p_o^{-2/3}}{p_o^{2/3}} = p_o^{-4/3} \tag{51}$$

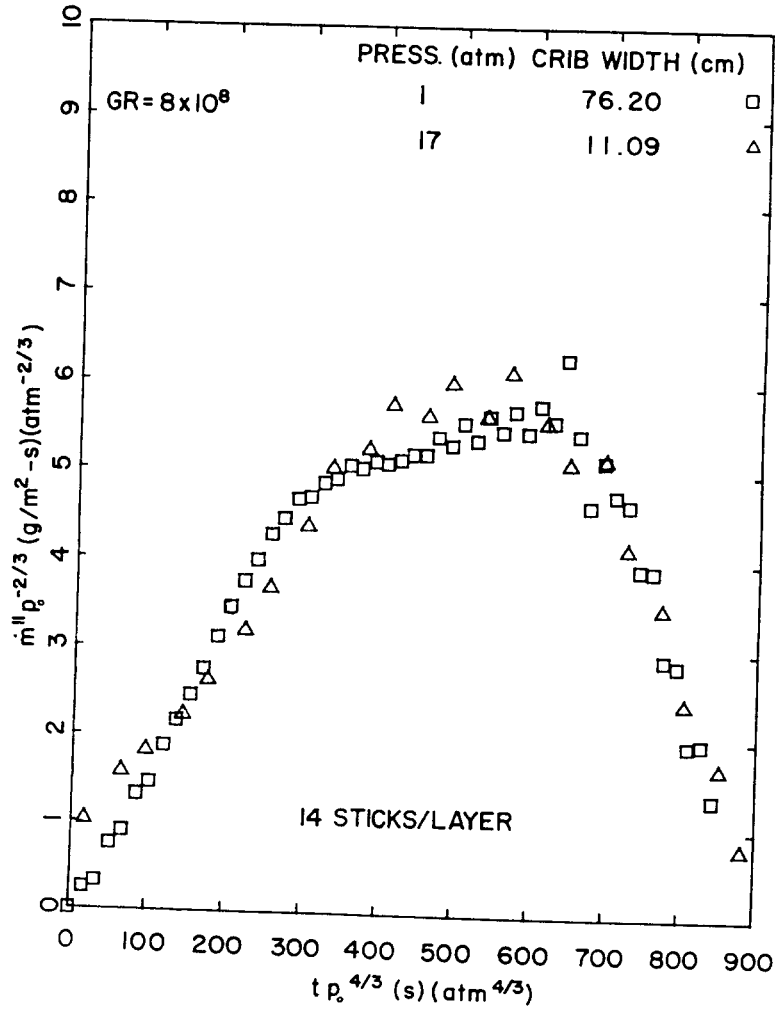


Fig. 6. Pressure modeling in the burning rate of wood cribs (from Alpert¹⁵).

since the crib geometric scales (l) is governed by eqn. (30). The success of pressure modeling to predict the transient burning of a crib is shown in Fig. 6.¹⁶ Block¹⁷ conducted a detailed study of the burning rate of wood cribs which led to a correlation in dimensionless variables which accounted for the crib geometric variables. Developed from small scale experiments (cribs generally of less than 1 ft high), the results were successfully extrapolated to predict the burning rate of wood pallet fires up to 12 ft high.

Emori and Saito¹⁸ investigated Froude modeling for radiation dominated ('large') pool fires and crib fires. They showed that scaling requires

$$\sigma T_f^4 l^2 / \dot{m} = \text{constant} \quad (52)$$

for a given fuel and configuration. This says that the energy radiation is a constant fraction of the combustion energy, $\dot{m}\Delta H$. Equation (52) follows for radiative dominated ($\kappa l \rightarrow 1$) steady burning from eqn. (17).

FLAME SPREAD

Alpert^{19,20} used pressure modeling to investigate upward flame spread on materials. For materials which propagated under normal atmospheric conditions, the results were good in that pyrolysis and flame lengths could be correlated with time as follows:

$$xa^{2/3} \text{ vs } ta^{4/3} \quad (53)$$

in which the length scale follows from eqn. (30) and the time scale from eqn. (51). The scaling law did not apply for materials that did not support spread under a normal atmosphere. In these cases, spread did occur at elevated pressure probably due to pressure enhanced flame radiation.

ENCLOSURE FIRES

Heskestad²¹ and Croce²² investigated steady-state conditions in enclosure fires with a wood crib fuel source. The rationale for their scaling criteria is explained as follows:

- (1) The burning rate (\dot{m}) of the crib in the enclosure depends on its free burn rate (\dot{m}_o), and the enclosure temperatures and oxygen concentration.

$$\frac{\dot{m}}{\dot{m}_o} = f_g(\hat{m}_o, \hat{T}, \hat{T}_s, Y_{O_2}) \quad (54)$$

where

$$\dot{m}_o \equiv \frac{\dot{m}_o}{Cb^{1/2}A_s} = f_{10}(P) \quad (55)$$

and b is stick thickness, A_s is exposed crib surface area, C is a dimensional constant and P is the crib porosity defined by Heskestad²¹ as a function of the crib design.

- (2) The thermal and concentration field of the enclosure depends on enclosure geometry, source of energy and specie, and enclosure boundary properties. From the governing equations (11–16) and boundary condition (21), applying Froude modeling and neglecting radiation gives

$$\{\hat{T}, \hat{T}_s, Y_i\} = f_{11}\left(\hat{Q}, \hat{x}, \frac{h\delta}{k_s}, \frac{\rho_s c_s \delta^2}{k_s \tau}\right) \quad (56)$$

where \hat{Q} is given in terms of $\dot{m}\Delta H$, and \hat{M}_i is implicit since \hat{M}_i can be related to \hat{Q} by stoichiometry, i.e.

$$\hat{M}_i = c_p T_o r_i \hat{Q} / \Delta H$$

where r_i is mass of i created per mass of fuel consumed.

By combining eqns. (54–56) it follows that

$$\left\{ \begin{array}{l} \hat{T} \\ \hat{T}_s \\ Y_i \\ \dot{m}/\dot{m}_o \end{array} \right\} = \text{function}\left(P, \frac{\dot{m}_o}{\rho_o c_p T_o \sqrt{g} l^{5/2}}, \frac{h\delta}{k_s}, \frac{\rho_s c_s \delta^2}{k_s \tau}, \hat{x}\right) \quad (57)$$

where \hat{x} implies coordinates and enclosure geometry, and τ is selected from the burn time, $\tau = (\text{mass of crib})/\dot{m}_o$. Heskestad²¹ designed his cribs to be geometrically similar and have $\dot{m}_o \propto b^2$ or $\dot{m}_o \propto m_o^{2/3}$, where m_o is the initial mass of the crib. In both cases^{21,22} some compromises must be made to satisfy all of the π -groups in eqn. (57). To match the enclosure conduction terms, different boundary materials were selected for the various scale systems. Figure 7 shows Heskestad's steady gas concentrations results for two similar enclosures, 48 and 98 cm high each, as a function of $l^{5/2}/\dot{m}_o$ represented as $A_o \sqrt{H_o}/m_o^{2/3}$ where A_o and H_o are the area and height of the enclosure window, respectively. Figure 8 shows Croce's²² results for wall surface temperature increase as a function of the same parameter for three enclosure sizes. The crib porosity, P , values were maintained equivalent in both sets of experiments.

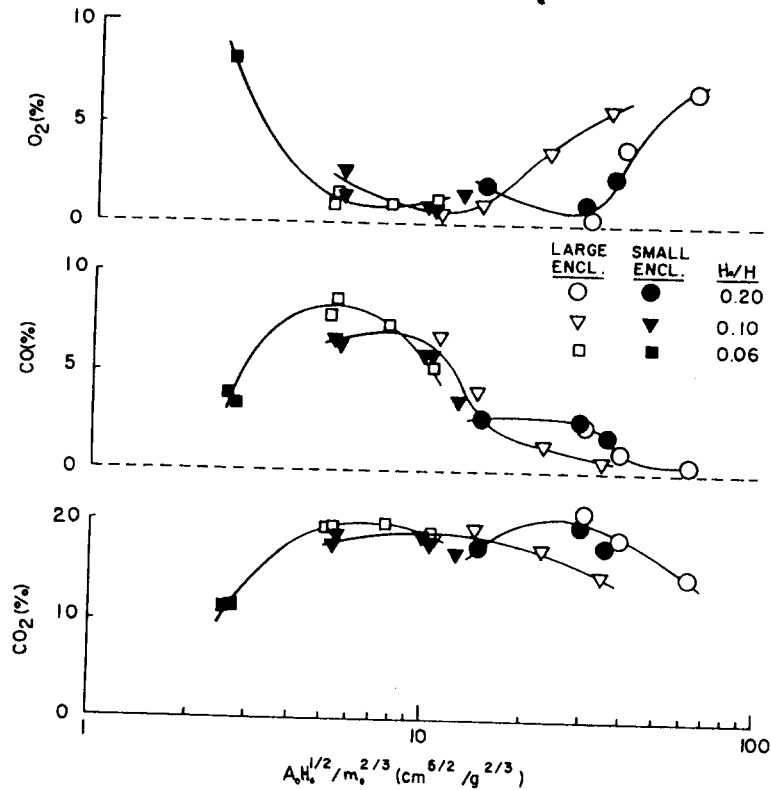


Fig. 7. Scaling in enclosure fires steady gas composition (from Heskestad²¹).

A practical design use of scale modeling was illustrated by Heskestad²³ in which he built a scale model of the Factory Mutual large-scale fire test facility. The model was used to determine more accurately the capacity of the air pollution equipment needed for the building exhaust—it confirmed that the contractor's estimate was $\frac{1}{3}$ th of the required flow rate.

A scaling study of the effect of a room fire on an adjoining corridor was done following a similar approach as suggested by eqn. (57).²⁴ Instead, however, the $\frac{1}{3}$ th scale model used a prescribed gas fuel supply source to reproduce the full-scale crib fires. Froude modeling was applied, with π_1 ignored (quasi-steady in the gas-phase), $\pi_2 = 1$ and π_3 , π_6 , π_7 and π_8 ignored. The scaling addressed

$$\left\{ \begin{array}{l} \hat{T} \\ \hat{T}_s \\ u/V \end{array} \right\} = \text{function} \left(\hat{x}, \hat{Q}, \frac{k_s \delta}{h}, \frac{(\rho c/k)_s \delta^2}{\tau} \right) \quad (58)$$

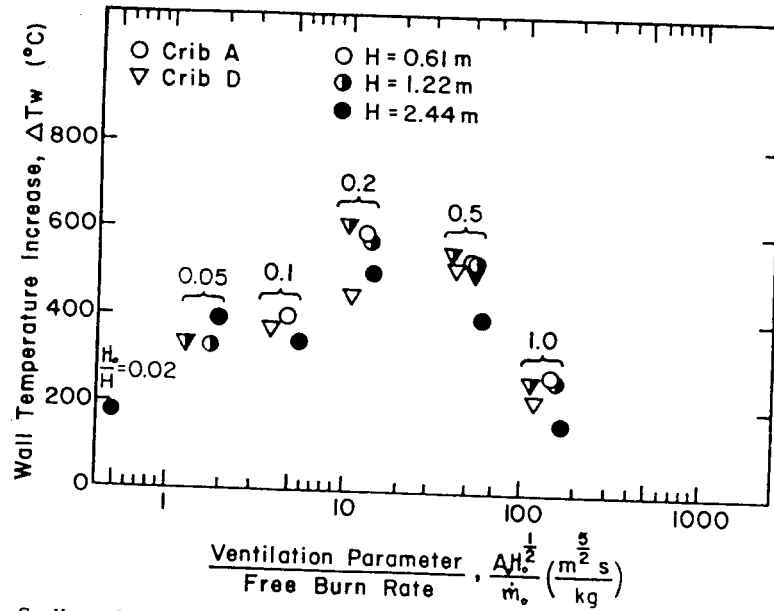


Fig. 8. Scaling of wall surface temperatures in steady enclosure fires (from Croce²²).

where τ was taken as the burn time, and h was taken $\propto l^{0.2}$ following eqn. (20). Enclosure construction materials were selected to insure matching of the corresponding π -terms. An example of the temperature results at several vertical positions in the corridor is shown in Fig. 9.

Other examples are given^{25,26} of room-corridor scale modeling which serve not only to confirm scaling, but to display and explore phenomenological behavior more conveniently in the smaller system. Moreover, Tanaka²⁷ has used a scale model of a two-story building to assess the accuracy of his mathematical model. Also, McCaffrey *et al.*²⁸ examined a wide range of enclosure fire data at several scales and constructions to arrive at a dimensionless correlation for maximum gas temperature. The results, surprisingly, nearly follow from the Boussinesq-based eqn. (23) with a consideration of eqn. (21) boundary condition ignoring radiation

$$\frac{T - T_o}{T_o \zeta} = f_{12} \left(\frac{Nu}{\pi_{13}} \right) = f_{12} \left(\frac{h \delta}{k_s} \right) \quad (59)$$

where

$$\zeta = \left(\frac{\dot{Q}}{\rho_o c_p T_o \sqrt{g} l^{5/2}} \right)^{2/3} \quad (60)$$

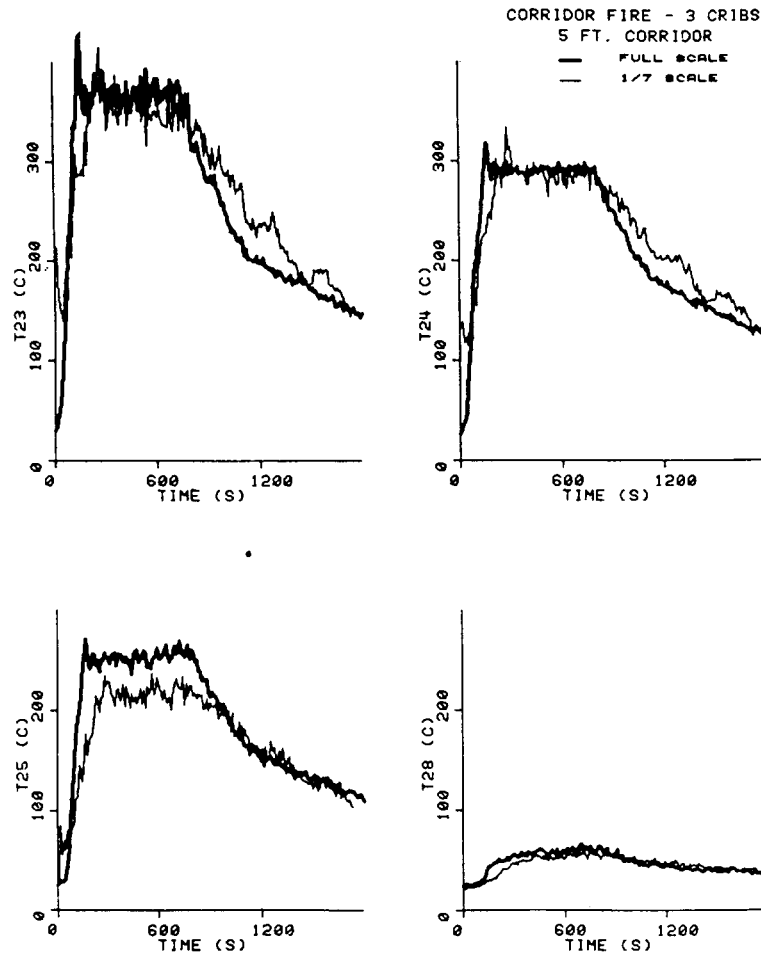


Fig. 9. Froude modeling in room-corridor fires—corridor vertical gas temperature distribution.²⁴

from eqns. (24–27). The correlation was found as

$$\frac{T - T_o}{T_o} = 1.6 \left(\frac{\dot{Q}}{\rho_o c_p T_o \sqrt{g} A_o \sqrt{H_o}} \right)^{2/3} \left(\frac{h_k A_s}{\rho_o c_p \sqrt{g} A_o \sqrt{H_o}} \right)^{-1/3} \quad (61)$$

where h_k is an effective heat transfer coefficient;²⁸ A_s , the enclosure surface area; A_o , the enclosure vent area; and H_o , the vent height.

An analog scaling study of a room corridor system was used to investigate the time for smoke filling.²⁹ The scale model used a dyed salt water source into fresh water to track the smoke front. Following eqns. (23–27), the position of the dimensionless smoke front, \hat{x} , is only a function of t/τ where $\tau = l/V$ and V is given by eqn. (27a)

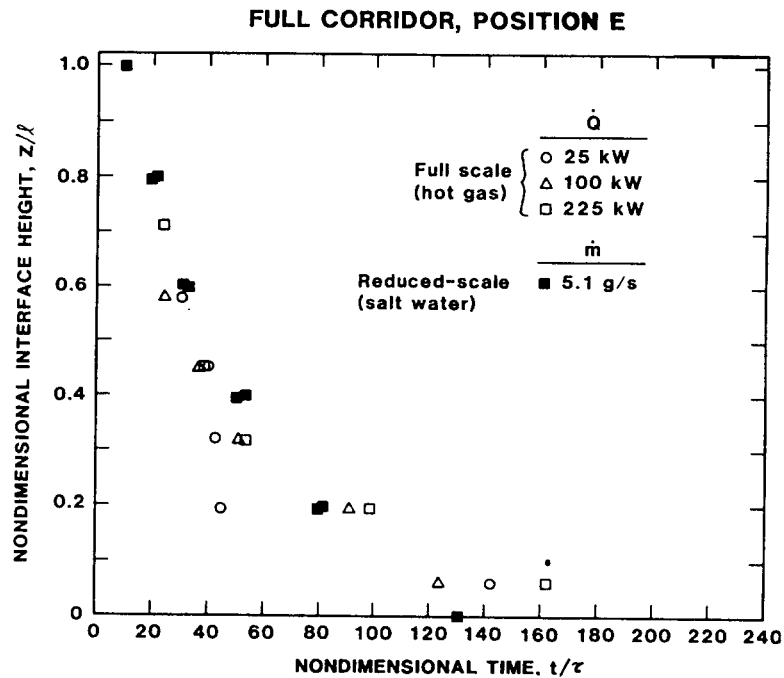


Fig. 10. Analog of corridor smoke filling.²⁹

for the fire system and eqn. (27b) for the salt water analog system with \dot{m}_i , the salt water flow rate. An example of the results is shown in Fig. 10.

ENCLOSURE FIRE GROWTH

A number of scale model studies based on Froude modeling have been performed to predict fire growth within an enclosure.³⁰⁻³³ These have been concerned with flame spread on the interior walls and ceiling of the enclosure. Despite the fact that complete scaling is not possible, these studies have met with limited success. A more specific examination of the mathematical modeling for this problem leads to 16 independent π -groups.³⁴ The effect of radiation on flame spread and burning rate suggest $\dot{Q} \propto l^2$, but \dot{Q} must be $\propto l^{5/2}$ according to Froude modeling.

CONCLUSIONS

The complex nature of fire and the limitations of realistic scale studies make scaling techniques attractive. It has been shown that the basic

governing equations, even in simplified form, produce too many dimensionless groups to permit complete scaling. Froude modeling emphasizes the convective processes, pressure modeling allows diffusive effects to be included, and analog techniques have advantages for visualization and avoidance of combustion effects. In all cases, the scaling techniques are incomplete and do not model all of the phenomena consistent with the governing dimensionless groups. Where some effects are small, this is justified. In other cases, incomplete modeling strategies serve to guide and provide useful correlations. Indeed, many correlations have been developed through scaling experiments and careful considerations of the dominant dimensionless groups. This review has attempted to show where incomplete dimensionless analyses have been successful, and where scale models have produced useful results and insight into fire behavior.

REFERENCES

1. Thomas, P. H., *Fire Safety Journal*, **5** (1983) 181–90.
2. Williams, F. A., *Fire Res. Abstracts and Rev.*, **11** (1969) 1–22.
3. Heskestad, G., *J. Fire and Flammability*, **6** (July 1975) 253–273.
4. Hottel, H. C., Fire Modeling. *The Use of Models in Fire Research*, Publication 786 National Academy of Sciences—NRC, Washington, DC, 1961, pp. 32–47.
5. McCaffrey, B. J., Purely Buoyant Diffusion Flames: Some Experimental Results, NBSIR 79-1919, National Bureau of Standards, October, 1979.
6. Taylor, G. I., Fire Under Influence of Natural Convection. In *The Use of Models in Fire Research*, Publication 786, National Academy of Sciences—NRC, Washington, DC, 1961, pp. 10–31.
7. Yokoi, S., Upward Convection Current From a Burning Wooden House. In *The Use of Models in Fire Research*, Publication 786, National Academy of Sciences—NRC, Washington, DC, 1961, pp. 186–206.
8. McCaffrey, B. J., Fire Plume Dynamics—A Review, Conference on Large Scale Fire Phenomenology, National Bureau of Standards, Gaithersburg, MD, September 10–13, 1984.
9. Heskestad, G., *Fire Safety Journal*, **5** (1983) 103–8.
10. Emori, R. I. & Saito, K., *Fire Technol.*, **18** (1982) 319–26.
11. Alpert, R. L., Fire Induced Turbulent Ceiling Jet, FMRC Ser. No. 19722-2, Factory Mutual Research, Norwood, MA, May, 1971.
12. Heskestad, G. & Delichatsios, M. A., The Initial Convective Flow in Fire, 17th Symp. (Int.) on Combustion, The Combustion Institute, Pittsburgh, PA, 1978, pp. 1113–23.
13. deRis, J., Kanury, A. M. & Yuen, M. C., Pressure Modeling of Fires, 14th Symp. (Int.) on Combustion, The Combustion Institute, Pittsburgh, PA, 1973, pp. 1033–43.

14. Kanury, A. M., Modeling of Pool Fires with a Variety of Polymers, 15th Symp. (Int.) on Combustion, The Combustion Institute, Pittsburgh, PA 1975, pp. 193-202.
15. Alpert, R. L., Pressure Modeling of Fires Controlled by Radiation, 16th Symp. (Int.) on Combustion, The Combustion Institute, Pittsburgh, PA, 1977, pp. 1489-1500.
16. Alpert, R. L., *Combustion Science and Technology*, **27**, (1976) 51-63.
17. Block, J. A., A Theoretical and Experimental Study of Nonpropagating Crib Fires, 13th Symp. (Int.) on Combustion, The Combustion Institute, Pittsburgh, PA, 1971, 971-8.
18. Emori, R. I. and Saito, K., *Combustion Science and Technology*, **31** (1983) 217-31.
19. Alpert, R. L., Pressure Modeling of Upward Fire Spread, FMRCJ.I.OAOR8.BU, Factory Mutual Research, Norwood, MA, March, 1979.
20. Alpert, R. L., Pressure Modeling of Fire Growth on Char-Forming Laminated Materials, FMRCJ.I.OGON3.BU, Factory Material Research, Norwood, MA, December, 1983.
21. Heskestad, G., Modeling of enclosure Fires, 14th Symp. (Int.) on Combustion, The Combustion Institute, Pittsburgh, PA, 1973, pp. 1021-30.
22. Croce, P. A., Modeling of Vented Enclosure Fires Part 1. Quasi-Steady Wood-Crib Source Fires, FMRCJ.I.7AOR5.GO, Factory Mutual Research, Norwood, MA, July, 1978.
23. Heskestad, G., Determination of Gas Venting Geometry and Capacity of Air Pollution Control System at Factory Mutual Research Center, FMRC Ser. No. 20581, Factory Mutual Research, Norwood, MA, November, 1972.
24. Quintiere, J., McCaffrey, B. J. & Kashiwagi, T., *Combustion Science and Technology*, **18** (1978) 1-19.
25. McCaffrey, B. J. & Quintiere, J. G., Buoyancy Driven Countercurrent Flows Generated by a Fire Source, In *Heat Transfer and Turbulent Buoyant Convection*, Vol. 2, ed. D. B. Spalding & N. Afgan, Hemisphere Publishing Corp., New York, 1976, pp. 457-72.
26. Quintiere, J. G., McCaffrey, B. J. & Rinkinen, W., *Fire and Materials*, **2** (1978) 18-24.
27. Tanaka, T., A Model on Fire Spread in Small Scale Buildings, 2nd Report, BRI Res., Paper No. 84, Building Research Institute, Japan, March, 1980.
28. McCaffrey, B. J., Quintiere, J. G. & Harkleroad, M., *Fire Technol.*, **17** (May, 1981) 90-108.
29. Steckler, K. D., Baum, H. R. & Quintiere, J. G., Salt Water Modeling of Fire Induced Flows in Multi-Compartment Enclosures, 21st Symp. (Int.) on Combustion, The Combustion Institute, Pittsburgh, PA, 1986, pp. 143-9.
30. Waterman, T. E., Scaled Room Flashover, IIT Res. Inst. OCD Work Unit 2534G, April, 1971.
31. Delichatsios, M. A., Corner Test Modeling, FMRC Ser. No. 22561, Factory Mutual Research, Norwood, MA, August, 1978.

32. Parker, W. J., An assessment of Correlations Between Laboratory and Full Scale Experiments for the FAA Aircraft Fire Safety Program, Part 6: Reduced-Scale Modeling of Compartments at Atmospheric Pressure, NBSIR 82-2598, National Bureau of Standards, March, 1983.
33. Kanury, A. M., Scaling Correlations of Flashover Experiments, NBS-GCR-83-448, National Bureau of Standards, October, 1983.
34. Quintiere, J. G., Significant Parameters for Predicting Flame Spread, NBSIR 85-3109, National Bureau of Standards, February, 1985.